LGR4 Maintains HGSOC Cell Epithelial Phenotype and Stem-Like Traits

Zhuo Wang
China Medical University
Ping Yin
China Medical University
Yu Sun
China Medical University
Lei Na
China Medical University
Jian Gao
China Medical University
Wei Wang
China Medical University
Chenghai Zhao (chzhao@cmu.edu.cn)
China Medical University https://orcid.org/0000-0003-2246-1425

Research

Keywords: ELF3, FZD5, LGR4, Ovarian cancer, WNT7B

Posted Date: June 12th, 2020

DOI: https://doi.org/10.21203/rs.3.rs-34651/v1

Version of Record: A version of this preprint was published at Gynecologic Oncology on December 1st, 2020. See the published version at https://doi.org/10.1016/j.ygyno.2020.09.020.

Abstract

Background: High-grade serous ovarian cancer (HGSOC) is lethal mainly due to extensive metastasis. Cancer cell stem-like properties are responsible for HGSOC metastasis. LGR4, a G-protein-coupled receptor, is involved in the maintenance of stem cell self-renewal and activity in some human organs.

Methods: TCGA and CCLE database was interrogated for gene mRNA analysis in ovarian cancer tissues and cell lines. The interactions between LGR4 and ELF3 were validated through dual-luciferase reporter assays, Chip assays and Co-IP assays. Gain- and loss-of functions of LGR4, ELF3, FZD5 and WNT7B were performed to identify their roles in the behaviors of ovarian cancer cells. Flowcytometry analysis and tumorisphere formation assays were performed to identified their stem-like properties. In vivo experiments were performed as well.

Results: LGR4 was shown to be overexpressed in HGSOCs and maintain the epithelial phenotype of HGSOC cells. LGR4 knockdown suppressed POU5F1, SOX2, PROM1 (CD133) and ALDH1A2 expression. Furthermore, LGR4 knockdown reduced CD133+ and ALDH+ subpopulations and impaired tumorisphere formation. To the contrary, LGR4 overexpression enhanced POU5F1 and SOX2 expression and tumorisphere formation capacity. LGR4 knockdown inhibited HGSOC cell growth and peritoneal seeding in xenograft models. Mechanistically, LGR4 and ELF3, an epithelium-specific transcription factor, formed a reciprocal regulatory loop, which was positively modulated by WNT7B/FZD5 pair. Consistently, knockdown of ELF3, WNT7B, and FZD5, respectively, disrupted HGSOC cell epithelial phenotype and stem-like properties.

Conclusion: Together, these data demonstrate that WNT7B/FZD5-LGR4/ELF3 axis maintains HGSOC cell epithelial phenotype and stem-like traits; targeting this axis may prevent HGSOC metastasis.

Background

Epithelial ovarian cancer (EOC) is the most lethal gynaecological cancer. Most EOC patients present at an advanced stage with extensive metastasis in the abdominal cavity, leading to the high mortality-to-incidence rate. Serous EOCs consist of high-grade serous ovarian cancers (HGSOCs) and low-grade serous ovarian cancers (LGSOCs), and HGSOCs account for 75% of all EOCs(1). EOC patients usually relapse after surgery in combination with chemotherapy. Recurrence is incurable because of rapid progression and therapy resistance.

Cancer cell stem-like properties contribute to EOC metastasis, recurrence and chemoresistance. Some cancer stem cell-related factors have been identified in EOC cells such as aldehyde dehydrogenase-1 (ALDH1), CD133 (PROM1) and CD44. Actually, these markers are functional. ALDH1, CD133 and CD44 all can endow EOC cells with stem-like properties and induce metastasis(2–5). Moreover, transcription factors OCT4 (POU5F1), SOX2 and NANOG are also involved in the generation of EOC stem cells(6).

LGR4, also known as GPR48, a G-protein-coupled receptor, plays an oncogenic role in human cancers. LGR4 overexpression promotes tumor metastasis and progression(7–9). LGR4 is involved in the maintenance of stem cell self-renewal and activity in intestine, mammary gland and prostate(10–13). Therefore, LGR4 is potentially associated with cancer stem cells. In the present study, LGR4 was identified to maintain HGSOC cell epithelial phenotype and stem-like traits. LGR4 knockdown suppressed HGSOC cell growth in vitro and in vivo. Furthermore, LGR4 knockdown interfered with HGSOC cell peritoneal seeding.

Methods

Patient specimens: Clinical specimens were collected from Liaoning Cancer Hospital & Institute with the informed consent of the patients. 29 HGSOCs, 5 LGSOCs and 8 normal ovary tissues were used. The normal ovary tissues were from the other side ovary of the patients. The use of these specimens for research purposes was approved by Institutional Research Ethics Committee of China Medical University.

Immunohistochemistry: Immunohistochemical staining was performed on 4-μm sections of paraffin-embedded tissues. Xylene and gradient alcohol were used to deparaffinize and hydrate, respectively. 3% H_2O_2 was used to eliminate endogenous peroxidase activity. Sections were then incubated with citrate buffer to repair antigen, and blocked by BSA. Primary antibody was added overnight at 4℃. After incubation with corresponding second antibody, sections were stained with DAB. Subsequently, sections were re-stained with hematoxylin and dehydrated with gradient alcohol and xylene. For human specimens, protein expression was scored according to H-scoring method. The scoring formula was H-score=ΣPi*i, where "I" represents the intensity of staining (0-3), and "Pi" stands for the percentage of stained tumor cells (0%-100%). For xenograft tumors, the positive staining tumor cells in 5 randomly selected fields were counted. Primary antibodies were used as follows: LGR4 (Abcam, UK); ELF3 and Cleaved caspase-3 (Cell Signaling Technology, USA); Ki67 (Invitrogen, USA).

In silico analysis: The Cancer Genome Atlas (TCGA) database was interrogated for LGR4 mRNA expression in ovarian cancer tissues. Cancer Cell Line Encyclopedia (CCLE) database was interrogated for gene mRNA expression in a panel of ovarian cancer cell lines. Correlation between two genes was analyzed using Pearson statistics. Heat maps were generated by GraphPad Prism 8.0.

Cell culture and transfection: Human ovarian cancer cell lines OVCAR3 and CAOV3, and HEK293T cells were grown in DMEM medium with 10% fetal bovine serum and 1% penicillin/streptomycin at 37℃ and 5% CO_2 in a humidified incubator. 2.5×10^5 cells were transiently transfected with shRNA or overexpression plasmids using Lipofectamine 3000 in Opti-MEM medium according to the product manual. 5×10^4 cells were transfected with shRNA lentiviruses to stably knockdown gene expression, and the transfected cell were further selected using 2μg/ml puromycin.

Real-time PCR: Total RNA from cells was extracted using TRIZOL reagent (Takara, China) according to the manufacturer's instruction. 1μg RNA was used to perform reverse transcription with the cDNA

synthesis Kit (Takara, China). The target cDNA was amplified with gene-specific primers using TB Green™ Premix Ex Taq II (Takara, China) and an ABI PRISM 7300 Sequence Detection system (Applied Biosystems, USA). The $2^{-\Delta\Delta Ct}$ analysis method was used for measuring relative gene expression. GAPDH was used as internal control. The primers used were as follows: LGR4 forward primer: CACACTTGGGCCAATAACTAAC, reverse primer: ACAAAGTCTTT TGCTGCTAAGG; FZD5 forward primer: TCCTCTGCATGGATTACAACC, reverse primer: GAC ACTTGCACACGAACG; WNT7B forward primer: GCAAGTGGATTTTCTACGTGTT; reverse primer: ATCTTGTTGCAGATGATGTTGG; ELF3 forward primer: ATGGTTTTCGTG ACTGCAAGAA, reverse primer: CAGTACTCTTTGCACAGCTTTC; OCT4 forward primer: GATGTGGTCCGAGTGTGGTTCTG, reverse primer: CGAGGAGTACAGTGCAGTGAAGTG; SOX2 forward primer: ACATGAACGGCTGGAGCAACG, reverse primer: CTGCGAGCTGG TCATGGAGTTG; PROM1 forward primer: GTGGCGTGTGCGGCTATGAC, reverse primer: CCAACTCCAACCATGAGGAAGACG; ALDH1A2 forward primer: TGCTGATGCTGACTTG GACATTGC, reverse primer: CCGCTCCACGCTTCTTCTCAC; ZEB2 forward primer: TGACCTGCCACCTGGAACTCC, reverse primer: GGCGGTACTTGATGTGCTCCTTC.

Western blot: For the total protein extraction, cells were lysed in RIPA buffer containing 10% protease inhibitor on ice for 40 minutes. Protein fragments were centrifuged with 12,000g at 4℃ for 30minutes. Protein concentration was determined using a BCA protein assay kit. Protein lysate was operated by SDS-PAGE and transferred to polyvinylidene difluoride membranes (PVDF). Then 5% BSA was used for blocking. Membranes were incubation with various primary antibody at 4℃ overnight and with respective secondary antibodies. The primary antibodies are as follows: LGR4 (Abcam, UK); ELF3, FZD5, WNT7B, E-cadherin, Vimentin and GAPDH (Cell Signaling Technology, USA). ECL detection system and imaging system were used to analyze the signals.

Immunofluorescence: Cells were seeded in 6-well plates at 1×10^5/well. After incubation for 48 hours, the cells were washed with cold PBS, fixed with 4% formaldehyde, permeabilized with 0.5% Triton X-100, and then blocked with 5% donkey serum and 0.3% Triton X-100 in 1X PBS. Then the cells were incubated overnight at 4 °C with antibodies for E-cadherin (1:100, Cell Signaling Technology, USA) or Vimentin (1:200, Cell Signaling Technology, USA), followed by incubation with Alexa Fluor 488-conjugated anti-mouse IgG for 2 hours at room temperature in the dark. Subsequently, the nuclei were staining by DAPI for 5 minutes. Immunofluorescence results were observed under a Laser scanning confocal focus microscope.

Flowcytometry: ALDEFLUOR assay kit (StemCell Technologies, USA) was used to detect ALDH activity. In brief, cells were suspended in the ALDEFLUOR assay buffer containing an ALDH substrate and incubated for 45 minutes at 37°C. 1×10^6 cells were used to detect the fluorescence signals by Flowcytometry (BD Biosciences, USA). CD133 positive cells were detected by Flowcytometry according to the standard protocol. 1×10^6 cells were harvested and washed with 1×PBS solution for three times, followed by incubation with 1μg fluorescein isothiocyanate (FITC)-labeled antibody for CD133 (Cell Signaling Technology, USA) for 30 minutes. Cells were then washed twice and resuspended in 100μl fluorescence-activated cell sorting (FACS) buffer.

Tumorisphere formation: 1×10^3 cells were seeded in 6-well Attachment Surface Polystyrene culture plates (Corning Costar, USA). Cells were cultured in complete MammoCult™ Human Medium (STEMCELL Technologies, USA) at 37°C and 5% CO_2 for 12 days. Spheroids in 5 randomly selected fields were counted.

Cell viability: Cell viability was determined by CCK8 assay. Cells were seeded in 96-well plates at 2×10^3/well. After incubation for 48 hours, CCK8 agent (Dojindo Molecular Technologies, Japan) was added. The absorbance at 450 nm was measured by a microplate reader (Bio-Rad Laboratories, USA) at the indicated time.

Colony formation: 1×10^3 cells were seeded in 3.5cm plates. After incubation for 14 days, cells were fixed with paraformaldehyde for 15 minutes at room temperature and then dyed by crystal violet (Solarbio, China) for 30 minutes at 37°C. Subsequently, colonies were counted and photographed.

In vivo animal study: All animal experiments were in strict accordance with the institutional guidelines and approved by the Animal Ethics Committee of China Medical University. BALB/c nude mice (5-6 weeks of age, female, 18-20g) were purchased from Beijing Vital River Laboratory Animal Technology Co., Ltd. (Beijing, China). 1×10^6 cells were subcutaneously injected into bilateral flanks of the mice (n=5 per group). Tumor length and width were measured with a vernier caliper every 3 days. Tumor volume was calculated by the formula: $V=1/2\times length\times width^2$. For the peritoneal metastasis assay, 5×10^6 cells were intra-peritoneally (i.p.) injected into BALB/c nude mice (n=5 per group). 30 days after injection, visible metastases in abdominal cavity were counted.

Dual-Luciferase Reporter Assay: Wild-type and mutant ELF3 binding sites in LGR4 promoter were subcloned into PGL3-Basic dual-luciferase vector to construct ELF3-LGR4-WT and ELF3-LGR4-Mut plasmids, respectively. Then the plasmids were co-transfected with ELF3 overexpression plasmids into HEK293T cells or co-transfected with ELF3 shRNA plasmids into OVCAR-3 cells. After 48 hours, luciferase activity was measured by Dual-Luciferase Reporter Assay System (Promega, USA) according to the manufacturer's instructions. The primers used were as follows: ELF3-CDS forward primers: CCGGAATTCCGGGCCACCATGGCTGCAACC, reverse primers: TTGCGGCCGCAATCAGTTCCGACTCT; LGR4-promoter-WT forward primers: GGGTACCCAGGCTGAGGCAGGAGAATCACT, reverse primers: CCAAGCTTGGTGGTTC CCAAACCCCCG; LGR4-promoter-Mut forward primers: TTTACAATTTCTCGGTTATTTGTTC ATGACAGTTG, reverse primers: GTTAGTTTCTGTAATCGTTTCTTTAAGATCTCTTC.

Chromatin Immunoprecipitation (ChIP): ChIP assays were performed using a ChIP assay kit (Beyotime, China) according to the manufacturer's instructions. Briefly, Cells in 10cm plates were fixed for 10 minutes at 37 °C with 1% formaldehyde. 1.1ml glycine solution was subsequently added into the plates. To shear the chromatin, cells were treated with 1mM PMSF in SDS Lysis Buffer for 10 minutes at 4°C, followed by cell sonication for 15 minutes at 4°C. After a portion of the cross-linked chromatin was removed as input for the subsequent test, the remaining cell lysis was incubated with 1μg ELF3 (Cell

Signaling Technology, USA) antibody at 4°C overnight. Then protein A+G agarose was added to precipitate the target protein recognized by the ELF3 antibody for 1 hour at 4°C. IgG antibody was used as a negative control. The beads were then washed off and DNA was collected for subsequent Real-time PCR assays. The enrichment was indicated as % of input. The primers used were as follows: ELF3-LGR4-promoter forward primers: GATCACGCCACTGGACAC, reverse primers: CTAAATAGGCTTTCATCGT; GAPDH-chip forward primers: TACTAGCGGTTTTACGGGCG, reverse primers: TCGAACAGGAGGAG CAGAGAGCGA.

***Co-Immunoprecipitation (Co-IP)*:** Cells were harvested and lysed in RIPA buffer containing 10% protease inhibitor on ice for 40 minutes. Protein fragments were centrifuged with 12,000 g at 4℃ for 30minutes. 500μg protein extract was incubated overnight at 4 °C with 1μg anti-FZD5 (Santa Cruz, USA) or anti-IgG antibody (Santa Cruz, USA) on a rotator. 20μl protein A/G-agarose beads (Santa Cruz, USA) were added for crosslink. The samples were then centrifuged and washed three times with PBS. The beads were harvested and resuspended in 20μl of gel loading buffer. Western blot was subsequently performed.

***Statistical analysis*:** The data are expressed as mean±SD. GraphPad prism 8 was used to analyze the data. Differences were analyzed by Student's t test or one-way ANOVA. P value less than 0.05 was considered statistically significant.

Results

LGR4 is overexpressed in HGSOCs and maintains the epithelial phenotype of HGSOC cells. LGR4 expression was examined in serous EOCs (n = 34) and normal ovaries (n = 8). As shown by IHC, LGR4 was preferentially expressed in HGSOCs (n = 29), while no LGR4 expression was found in normal ovaries (Fig. 1A, 1B). Serous EOCs with metastasis at the time of diagnosis (n = 24) expressed more LGR4 compared with those without metastasis (n = 10) (Fig. 1C). Interrogation of TCGA database revealed that EOCs with grade 3 + 4 (n = 321) expressed more LGR4 mRNA than those with grade 1 + 2 (n = 43) (Fig. 1D). Interrogation of CCLE database revealed that LGR4 was positively correlated with epithelial factors, while negatively correlated with mesenchymal factors (Fig. 1E). Two HGSOC cell lines, OVCAR3 and CAOV3 with high and low LGR4 expression, respectively, were selected for the present study. Three LGR4 shRNA plasmids were used to transfect OVCAR3 cells. As shown by real-time PCR, LGR4 shRNA-2 transfection suppressed LGR4 mRNA expression most efficiently (Fig. 1F). Subsequently, OVCAR3 cells were stably transfected with LGR4 shRNA-2 lentivirus. LGR4 knockdown significantly reduced E-cadherin expression, whereas increased Vimentin expression (Fig. 1G, Supplementary Fig. 1A). LGR4 knockdown also increased ZEB2 expression (Supplementary Fig. 1B). To the contrary, LGR4 overexpression in CAOV3 cells elevated E-cadherin expression, but decreased Vimentin expression (Fig. 1H).

LGR4 contributes to HGSOC cell stem-like traits. OVCAR3 and CAOV3 cells have been demonstrated with high and low tumorigenicity, respectively(14). LGR4 knockdown in OVCAR3 cells inhibited expression of two stem cell-related transcription factors, POU5F1 and SOX2 (Fig. 2A). LGR4 knockdown also suppressed expression of PROM1 (CD133) and ALDH1A2 (Fig. 2A). Consistently, LGR4 knockdown

reduced ALDH + and CD133 + subpopulations, as shown by Flowcytometry (Fig. 2B, 2C). LGR4 knockdown had no effect on expression of CD44, a mesenchymal cancer stem cell marker (data not shown). Furthermore, LGR4 knockdown impaired tumorisphere formation of OVCAR3 cells (Fig. 2D). Neither CD133 + nor ALDH + subpopulation was detected by Flowcytometry in CAOV3 cells with LGR4 or control overexpression. However, LGR4 overexpression still enhanced POU5F1 and SOX2 expression and tumorisphere formation capacity (Fig. 2E, 2F).

LGR4 promotes HGSOC cell growth and peritoneal seeding. The role of LGR4 in HGSOC cell growth was investigated in vitro and in vivo. Both CCK8 and colony formation tests showed that LGR4 knockdown interfered with the growth of in vitro cultured OVCAR3 cells (Fig. 3A, 3B). Xenograft models using nude mice further demonstrated that LGR4 knockdown delayed the appearance and hampered the growth of OVCAR3 tumors (Fig. 3C). Moreover, xenograft tumors with LGR4 knockdown demonstrated reduced Ki67 expression, whereas increased cleaved caspase-3 expression (Fig. 3D). As epithelial stemness facilitates tumor cells to colonize in secondary sites, a peritoneal seeding model was adopted to evaluate the role of LGR4 in HGSOC metastasis. OVCAR3 cells with LGR4 knockdown formed less and smaller metastatic colonies in abdominal cavity compared with those with control knockdown (Fig. 3E).

LGR4 and ELF3 form a reciprocal regulatory loop. To inquire whether a link exists between LGR4 and ELF3, an epithelium-specific transcription factor, ELF3 expression was detected in HGSOCs by IHC. H-score statistics revealed a similar expression pattern of ELF3 to that of LGR4 (Fig. 4A, 4B). Interrogation of CCLE database further uncovered a positive correlation between LGR4 and ELF3 (Fig. 4C). LGR4 knockdown in OVCAR3 cells reduced ELF3 expression in both protein and mRNA levels (Fig. 4D, 4E). Intriguingly, ELF3 knockdown by ELF3 lentivirus transfection reversely suppressed LGR4 expression (Fig. 4F, 4G). As a member in ETS1 family of transcription factors, ELF3 specifically recognizes and binds to a core motif C/A GGA A/T (or T/A TCC G/T)(15–17). In combination with JASPAR database (http://jaspar.genereg.net/), an ELF3 binding site was identified on LGR4 promoter (Fig. 4H, 4I). Luciferase reporter assay confirmed the binding of exogenous ELF3 to the predicted sites in HEK293T cells (Fig. 4J). Moreover, Luciferase reporter assay showed that ELF3 knockdown in OVCAR3 cells reduced LGR4 promoter activity (Fig. 4K). Finally, ChIP and subsequent real-time PCR verified the binding of ELF3 to LGR4 promoter in OVCAR3 cells (Fig. 4L).

ELF3 is involved in HGSOC cell epithelial phenotype and stem-like traits. As shown by immunofluorescence, ELF3 knockdown in OVCAR3 cells suppressed E-cadherin expression, whereas elevated Vimentin expression (Fig. 5A, Supplementary Fig. 2). ELF3 knockdown increased ZEB2 expression as well (Fig. 5B). ELF3 knockdown reduced POU5F1, SOX2, PROM1 and ALDH1A2 expression (Fig. 5C), and CD133 + and ALDH + subpopulations (Fig. 5D, 5E). Similarly, ELF3 knockdown had no effect on CD44 expression (data not shown). Finally, ELF3 knockdown dampened tumorisphere formation of OVCAR3 cells (Fig. 5F). Just as expected, ELF3 overexpression in CAOV3 cells increased POU5F1 and SOX2 expression, and tumorisphere formation capacity (Supplementary Fig. 3A, 3B).

LGR4-ELF3 is modulated by WNT7B/FZD5 pair. Interrogation of CCLE database revealed that LGR4 and ELF3 were associated with WNT7B/FZD5 pair (Fig. 6A). Co-IP test confirmed the binding of WNT7B to FZD5 in OVCAR3 cells (Fig. 6B). Either WNT7B knockdown or FZD5 knockdown reduced LGR4 and ELF3 expression (Fig. 6C, 6D). WNT7B/FZD5 knockdown decreased active β-catenin expression, indicating that the binding of WNT7B to FZD5 can activate canonical Wnt/β-catenin pathway (Fig. 6E). However, LGR4 and ELF3 expression was suppressed by WNT inhibitor C59, but not affected by β-catenin inhibitor XAV939 (Fig. 6F, 6G), suggesting WNT7B/FZD5 pair modulated LGR4-ELF3 loop via non-canonical Wnt pathway. WNT7B/FZD5 knockdown in OVCAR3 cells inhibited E-cadherin, POU5F1, SOX2, PROM1 and ALDH1A2 expression (Fig. 7A-D). Moreover, WNT7B/FZD5 knockdown diminished ALDH + and CD133 + subpopulations and suppressed tumorisphere formation (Fig. 7E-H; Supplementary Fig. 4A, 4B).

Discussion

Based on the finding that LGR4 is preferentially expressed in HGSOCs, two HGSOC cell lines were selected for subsequent gain and loss of function study. On the one hand, LGR4 maintains the epithelial phenotype. LGR4 regulates E-cadherin positively, whereas Vimentin and ZEB2 negatively. This is further supported by CCLE database interrogation showing that LGR4 is correlated with a series of epithelial factors including not only CDH1 (E-cadherin), but also EPCAM, ELF3, CLDN2, CLDN3, KRT8 and KRT19. On the other hand, LGR4 maintains cancer cell stem-like properties. LGR4 affects POU5F1, SOX2, CD133 and ALDH1A2 expression and tumorisphere formation capacity. Notably, LGR4 has no effect on mesenchymal cancer stem cell marker CD44.

It was reported that breast cancer stem cells (BCSCs) exist in distinct mesenchymal and epithelial states(18, 19). Mesenchymal BCSCs are characterized by epithelial-mesenchymal transition (EMT), CD24-CD44+, quiescence and being at the tumor invasive front; while epithelial BCSCs are ALDH1+, proliferative, located more centrally and characterized by mesenchymal-epithelial transition (MET). Similarly, EOC stemness exhibits phenotypic and functional heterogeneity(20). Mesenchymal EOC stem cells express CD44, CD117 and TGF-β1(21, 22), while epithelial EOC stem cells are characterized by MET and prone to colonize at metastatic sites(23). Our study found that LGR4induces epithelial phenotype and stem-like properties which promotes EOC cell growth and peritoneal seeding.

ELF3 plays complicated roles in human cancers. ELF3 functions as a tumor suppressor in ampullary carcinoma(24, 25), but as an oncogene in lung adenocarcinoma(26, 27). There are even contradictory observations about the role of ELF3 in prostate cancer(28, 29). Yeung et al. reported that ELF3 is a negative regulator of EMT(30). This is consistent with our finding. However, our study revealed that ELF3 is implicated in EOC stem-like properties, potentially inducing EOC cell growth and metastasis through regulating LGR4. The association of LGR4-ELF3 with epithelial phenotype may be related to the suppression of ZEB2. ELF3 negatively regulates ZEB1/2 expression in breast cancer cells(31).

WNT7A was shown to promote EOC cell growth, invasion and migration via FZD5 in a β-catenin-dependent way(32, 33). Similarly, WNT7B/FZD5 pair was found to activate β-catenin pathway in our

study. However, WNT7B/FZD5 pair modulates LGR4 and ELF3 expression and maintains EOC cell stem-like properties independent on β-catenin. Therefore, WNT7B/FZD5 pair seems to be involved in EOC via both canonical and non-canonical Wnt pathways.

In summary, our study for the first time elucidated the role of LGR4 in HGSOC. LGR4 maintains HGSOC cell epithelial phenotype and stem-like traits, and promotes HGSOC cell growth and peritoneal seeding. Mechanistically, LGR4 and ELF3 form a reciprocal regulatory loop, which is modulated by WNT7B/FZD5 pair via non-canonical Wnt pathway. Furthermore, ELF3, WNT7B and FZD5 are also implicated in HGSOC cell epithelial phenotype and stem-like traits. Targeting these molecules may potentially suppress HGSOC growth and metastasis.

Abbreviations

HGSOC: High-grade serous ovarian cancer; EOC: Epithelial ovarian cancer; LGSOC: Low-grade serous ovarian cancers; ALDH1: Aldehyde dehydrogenase-1; BSA: Bull Serum Albumin; DAB: 3,3'-diaminobenzidine; GAPDH: Glyceraldehyde-3-phosphate dehydrogenase; RT-qPCR: reverse transcription quantitative polymerase chain reaction; Chip: Chromatin Immunoprecipitation; Co-IP : Co-Immunoprecipitation; IHC: Immunohistochemistry; BCSCs: breast cancer stem cells; EMT: epithelial-mesenchymal transition; MET: mesenchymal-epithelial transition; WT: wild type; MUT: mutant type.

Declarations

Ethics approval and consent to participate

The use of the specimens for research purposes was approved by Institutional Research Ethics Committee of China Medical University. All animal experiments were in strict accordance with the institutional guidelines and approved by the Animal Ethics Committee of China Medical University.

Consent for publication

Not applicable.

Availability of data and materials

Not applicable.

Competing interests

The authors declare that they have no competing interests.

Funding

No.

Authors' contributions

Conceptualization, C.Z.; methodology, Z.W., W.W., P.Y. Y.S. and J.G.; software, L.N.; data curation, Z.W.; writing—original draft preparation, Z.W.; writing—review and editing, C.Z.; supervision, C.Z.; project administration, C.Z. All authors have read and agreed to the published version of the manuscript.

Acknowledgements

Not applicable.

References

1. Lheureux S, Gourley C, Vergote I, Oza AM. Epithelial ovarian cancer. Lancet. 2019;393(10177):1240-53.
2. Yokoyama Y, Zhu H, Lee JH, Kossenkov AV, Wu SY, Wickramasinghe JM, et al. BET Inhibitors Suppress ALDH Activity by Targeting ALDH1A1 Super-Enhancer in Ovarian Cancer. Cancer research. 2016;76(21):6320-30.
3. Landen CN, Goodman B, Katre AA, Steg AD, Nick AM, Stone RL, et al. Targeting aldehyde dehydrogenase cancer stem cells in ovarian cancer. Molecular cancer therapeutics. 2010;9(12):3186-99.
4. Roy L, Bobbs A, Sattler R, Kurkewich JL, Dausinas PB, Nallathamby P, et al. CD133 Promotes Adhesion to the Ovarian Cancer Metastatic Niche. Cancer Growth Metastasis. 2018;11:1179064418767882.
5. Sacks Suarez J, Gurler Main H, Muralidhar GG, Elfituri O, Xu HL, Kajdacsy-Balla AA, et al. CD44 Regulates Formation of Spheroids and Controls Organ-Specific Metastatic Colonization in Epithelial Ovarian Carcinoma. Mol Cancer Res. 2019;17(9):1801-14.
6. Parte SC, Smolenkov A, Batra SK, Ratajczak MZ, Kakar SS. Ovarian Cancer Stem Cells: Unraveling a Germline Connection. Stem Cells Dev. 2017;26(24):1781-803.
7. Gao Y, Kitagawa K, Hiramatsu Y, Kikuchi H, Isobe T, Shimada M, et al. Up-regulation of GPR48 induced by down-regulation of p27Kip1 enhances carcinoma cell invasiveness and metastasis. Cancer research. 2006;66(24):11623-31.
8. van Andel H, Ren Z, Koopmans I, Joosten SPJ, Kocemba KA, de Lau W, et al. Aberrantly expressed LGR4 empowers Wnt signaling in multiple myeloma by hijacking osteoblast-derived R-spondins.

Proceedings of the National Academy of Sciences of the United States of America. 2017;114(2):376-81.

9. Kang YE, Kim J-M, Kim KS, Chang JY, Jung M, Lee J, et al. Upregulation of RSPO2-GPR48/LGR4 signaling in papillary thyroid carcinoma contributes to tumor progression. Oncotarget. 2017;8(70):114980-94.
10. Mustata RC, Van Loy T, Lefort A, Libert F, Strollo S, Vassart G, et al. Lgr4 is required for Paneth cell differentiation and maintenance of intestinal stem cells ex vivo. EMBO Rep. 2011;12(6):558-64.
11. Hilkens J, Timmer NC, Boer M, Ikink GJ, Schewe M, Sacchetti A, et al. RSPO3 expands intestinal stem cell and niche compartments and drives tumorigenesis. Gut. 2017;66(6):1095-105.
12. Wang Y, Dong J, Li D, Lai L, Siwko S, Li Y, et al. Lgr4 regulates mammary gland development and stem cell activity through the pluripotency transcription factor Sox2. Stem Cells. 2013;31(9):1921-31.
13. Luo W, Rodriguez M, Valdez JM, Zhu X, Tan K, Li D, et al. Lgr4 is a key regulator of prostate development and prostate stem cell differentiation. Stem Cells. 2013;31(11):2492-505.
14. Mitra AK, Davis DA, Tomar S, Roy L, Gurler H, Xie J, et al. In vivo tumor growth of high-grade serous ovarian cancer cell lines. Gynecol Oncol. 2015;138(2):372-7.
15. Wasylyk B, Hahn SL, Giovane A. The Ets family of transcription factors. Eur J Biochem. 1993;211(1-2).
16. Tymms MJ, Ng AY, Thomas RS, Schutte BC, Zhou J, Eyre HJ, et al. A novel epithelial-expressed ETS gene, ELF3: human and murine cDNA sequences, murine genomic organization, human mapping to 1q32.2 and expression in tissues and cancer. Oncogene. 1997;15(20):2449-62.
17. Sizemore GM, Pitarresi JR, Balakrishnan S, Ostrowski MC. The ETS family of oncogenic transcription factors in solid tumours. Nat Rev Cancer. 2017;17(6):337-51.
18. Liu S, Cong Y, Wang D, Sun Y, Deng L, Liu Y, et al. Breast cancer stem cells transition between epithelial and mesenchymal states reflective of their normal counterparts. Stem cell reports. 2014;2(1):78-91.
19. Beerling E, Seinstra D, de Wit E, Kester L, van der Velden D, Maynard C, et al. Plasticity between Epithelial and Mesenchymal States Unlinks EMT from Metastasis-Enhancing Stem Cell Capacity. Cell reports. 2016;14(10):2281-8.
20. Hatina J, Boesch M, Sopper S, Kripnerova M, Wolf D, Reimer D, et al. Ovarian Cancer Stem Cell Heterogeneity. Advances in experimental medicine and biology. 2019;1139:201-21.
21. Mitra T, Prasad P, Mukherjee P, Chaudhuri SR, Chatterji U. Stemness and chemoresistance are imparted to the OC cells through TGFbeta1 driven EMT. 2018;119(7):5775-87.
22. Zhang S, Balch C, Chan MW, Lai HC, Matei D, Schilder JM, et al. Identification and characterization of ovarian cancer-initiating cells from primary human tumors. Cancer research. 2008;68(11):4311-20.
23. Li Y, Gong W, Ma X, Sun X, Jiang H, Chen T. Smad7 maintains epithelial phenotype of ovarian cancer stem-like cells and supports tumor colonization by mesenchymal-epithelial transition. Molecular medicine reports. 2015;11(1):309-16.

24. Yachida S, Wood LD, Suzuki M, Takai E, Totoki Y, Kato M, et al. Genomic Sequencing Identifies ELF3 as a Driver of Ampullary Carcinoma. Cancer cell. 2016;29(2):229-40.
25. Gingras MC, Covington KR, Chang DK, Donehower LA, Gill AJ, Ittmann MM, et al. Ampullary Cancers Harbor ELF3 Tumor Suppressor Gene Mutations and Exhibit Frequent WNT Dysregulation. Cell reports. 2016;14(4):907-19.
26. Ali SA, Justilien V, Jamieson L, Murray NR, Fields AP. Protein Kinase Ciota Drives a NOTCH3-dependent Stem-like Phenotype in Mutant KRAS Lung Adenocarcinoma. Cancer cell. 2016;29(3):367-78.
27. Enfield KSS, Marshall EA. Epithelial tumor suppressor ELF3 is a lineage-specific amplified oncogene in lung adenocarcinoma. 2019;10(1):5438.
28. Shatnawi A, Norris JD, Chaveroux C, Jasper JS, Sherk AB, McDonnell DP, et al. ELF3 is a repressor of androgen receptor action in prostate cancer cells. Oncogene. 2014;33(7):862-71.
29. Longoni N, Sarti M, Albino D, Civenni G, Malek A, Ortelli E, et al. ETS transcription factor ESE1/ELF3 orchestrates a positive feedback loop that constitutively activates NF-kappaB and drives prostate cancer progression. Cancer research. 2013;73(14):4533-47.
30. Yeung TL, Leung CS, Wong KK, Gutierrez-Hartmann A, Kwong J, Gershenson DM, et al. ELF3 is a negative regulator of epithelial-mesenchymal transition in ovarian cancer cells. Oncotarget. 2017;8(10):16951-63.
31. Sinh ND, Endo K, Miyazawa K, Saitoh M. Ets1 and ESE1 reciprocally regulate expression of ZEB1/ZEB2, dependent on ERK1/2 activity, in breast cancer cells. 2017;108(5):952-60.
32. Yoshioka S, King ML, Ran S, Okuda H, MacLean JA, 2nd, McAsey ME, et al. WNT7A regulates tumor growth and progression in ovarian cancer through the WNT/beta-catenin pathway. Mol Cancer Res. 2012;10(3):469-82.
33. King ML, Lindberg ME, Stodden GR, Okuda H, Ebers SD, Johnson A, et al. WNT7A/beta-catenin signaling induces FGF1 and influences sensitivity to niclosamide in ovarian cancer. Oncogene. 2015;34(26):3452-62.

Figures

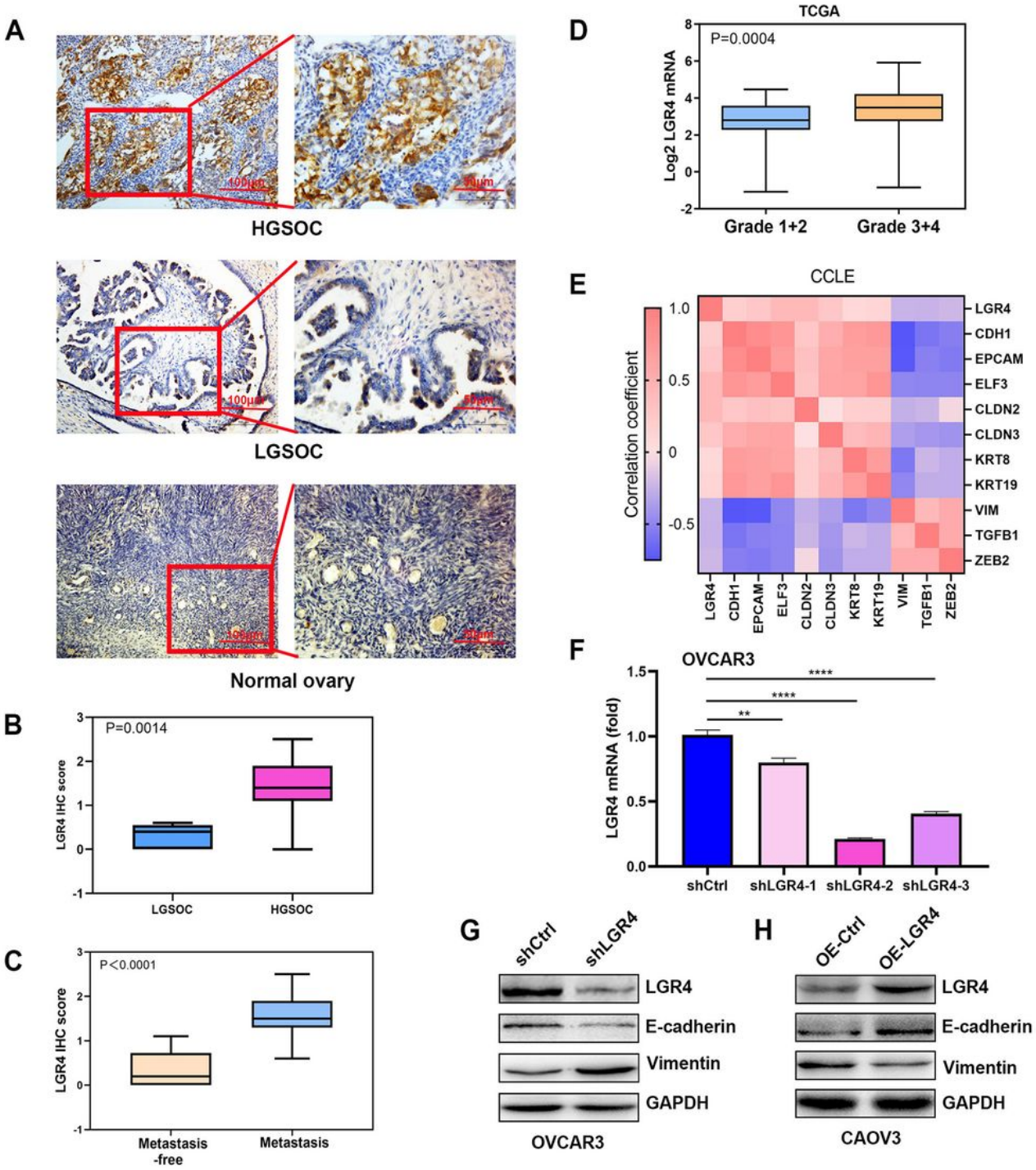

Figure 1

LGR4 is overexpressed in HGSOCs and maintains the epithelial phenotype of HGSOC cells. (A) LGR4 expression was detected in HGSOCs (n=29), LGSOCs (n=5) and normal ovaries (n=8) by Immunohistochemistry (IHC). (B) LGR4 expression was scored in LGSOCs (n=5) and HGSOCs (n=29). (C) LGR4 expression was scored in serous EOCs without metastasis (n=10) and those with peritoneal metastasis (n=24). (D) TCGA database was interrogated for LGR4 expression in Grade 1+2 (n=43) and

Grade 3+4 (n=321) ovarian cancers. (E) A heat map was generated from CCLE database. (F) LGR4 expression was detected in OVCAR3 cells transfected with Control shRNA or different LGR4 shRNAs by Real-time PCR. (G) LGR4, E-cadherin and Vimentin expression was detected in OVCAR3 cells transfected with Control shRNA or LGR4 shRNA by Western blot. (H) LGR4, E-cadherin and Vimentin expression was detected in CAOV3 cells transfected with Control vector or LGR4 overexpression (OE) vector by Western blot. Real-time and Western blot experiments were performed in triplicate. Error bars indicate SD. **P<0.01, ****P<0.0001.

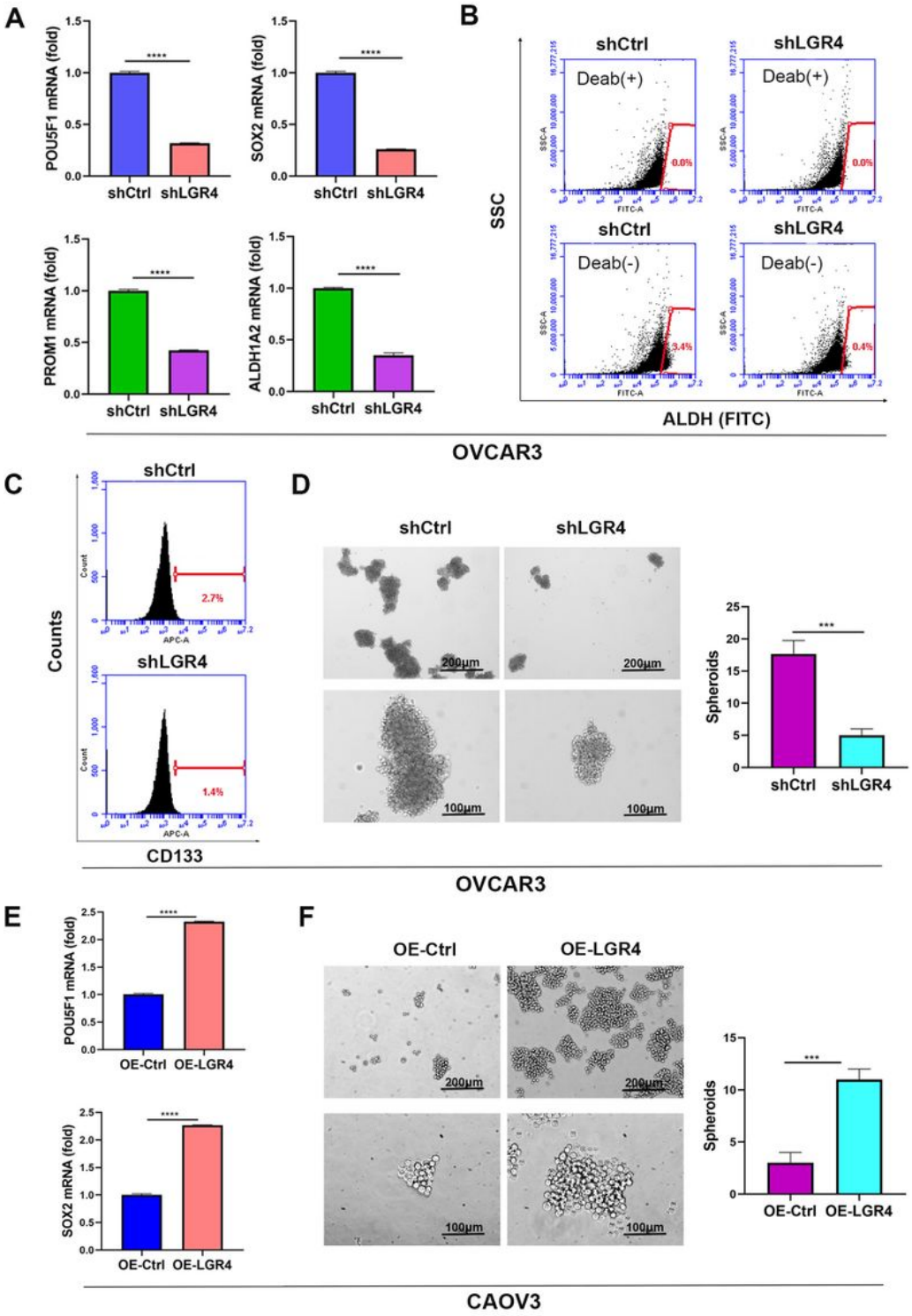

Figure 2

LGR4 contributes to HGSOC cell stem-like traits. (A) POU5F1, SOX2, PROM1 and ALDH1A2 expression was detected in OVCAR3 cells transfected with Control shRNA or LGR4 shRNA by Real-time PCR. (B) and (C) ALDH+ and CD133+ subpopulations were detected in OVCAR3 cells transfected with Control shRNA or LGR4 shRNA by Flowcytometry. (D) Spheroids per field were counted in OVCAR3 cells transfected with Control shRNA or LGR4 shRNA. (E) POU5F1 and SOX2 expression was detected in CAOV3 cells transfected with Control vector or LGR4 overexpression vector by Real-time PCR. (F) Spheroids per field were counted in CAOV3 cells transfected with Control vector or LGR4 overexpression vector. All experiments were performed in triplicate. Error bars indicate SD. ***P<0.001, ****P<0.0001.

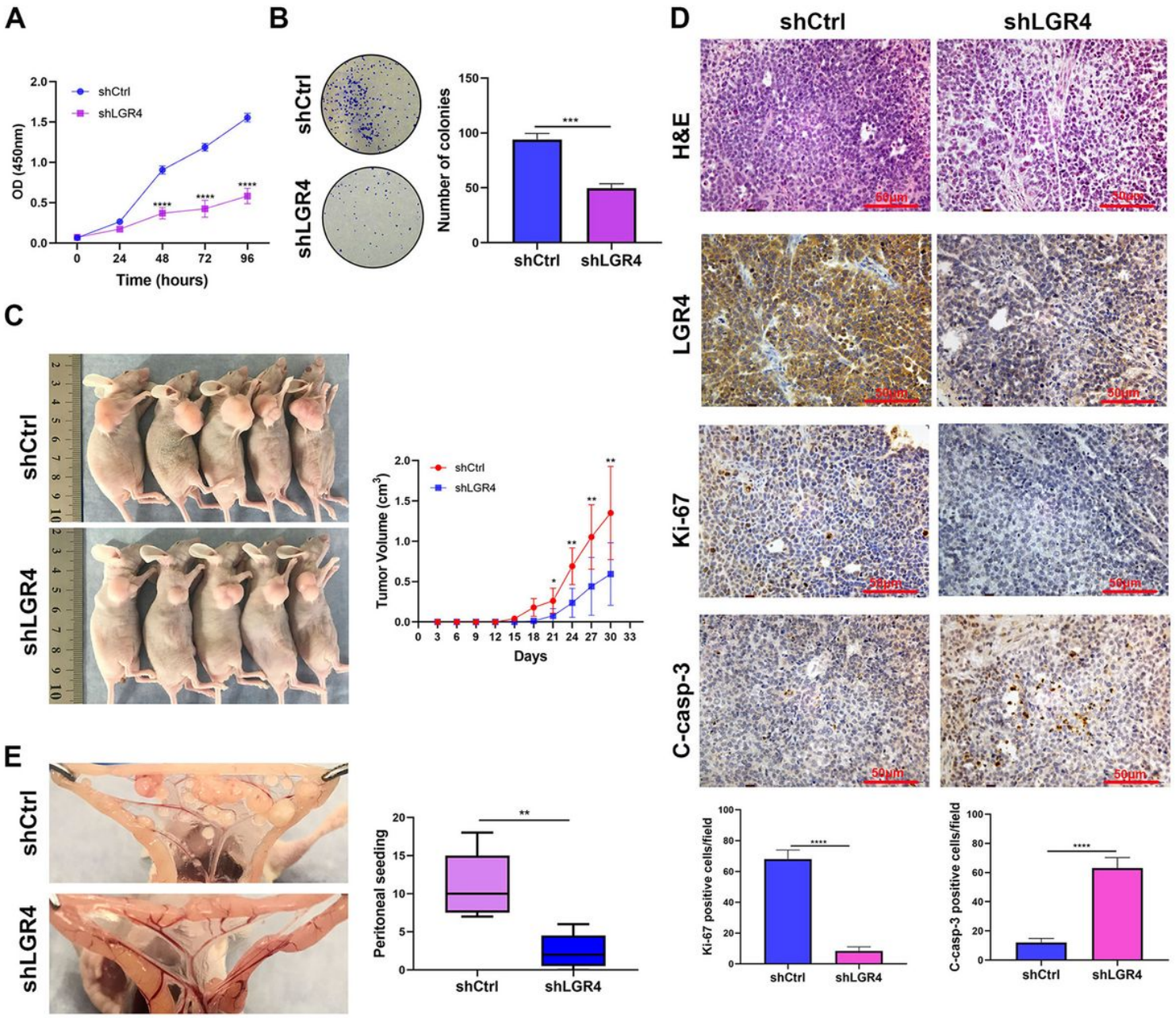

Figure 3

LGR4 promotes HGSOC cell growth and peritoneal metastasis. (A) and (B) Growth of OVCAR3 cells transfected with Control shRNA or LGR4 shRNA was in vitro analyzed by CCK-8 and colony formation tests. All experiments were performed in triplicate. (C) OVCAR3 cells transfected with Control shRNA or LGR4 shRNA were inoculated into nude mice (n=5 in each group). Tumor volume was calculated according to 1/2×length×width2. (D) Xenograft tumors were confirmed by HE staining. LGR4, Ki67 and cleaved caspase-3 (C-casp-3) expression was detected in xenograft tumors by IHC. (E) OVCAR3 cells transfected with Control shRNA or LGR4 shRNA were seeded into peritoneal cavity of nude mice (n=5 in each group). Mesenteric colonies were shown here and visible metastases in abdominal cavity were counted. Error bars indicate SD. *P<0.05, **P<0.01, ***P<0.001, ****P<0.0001.

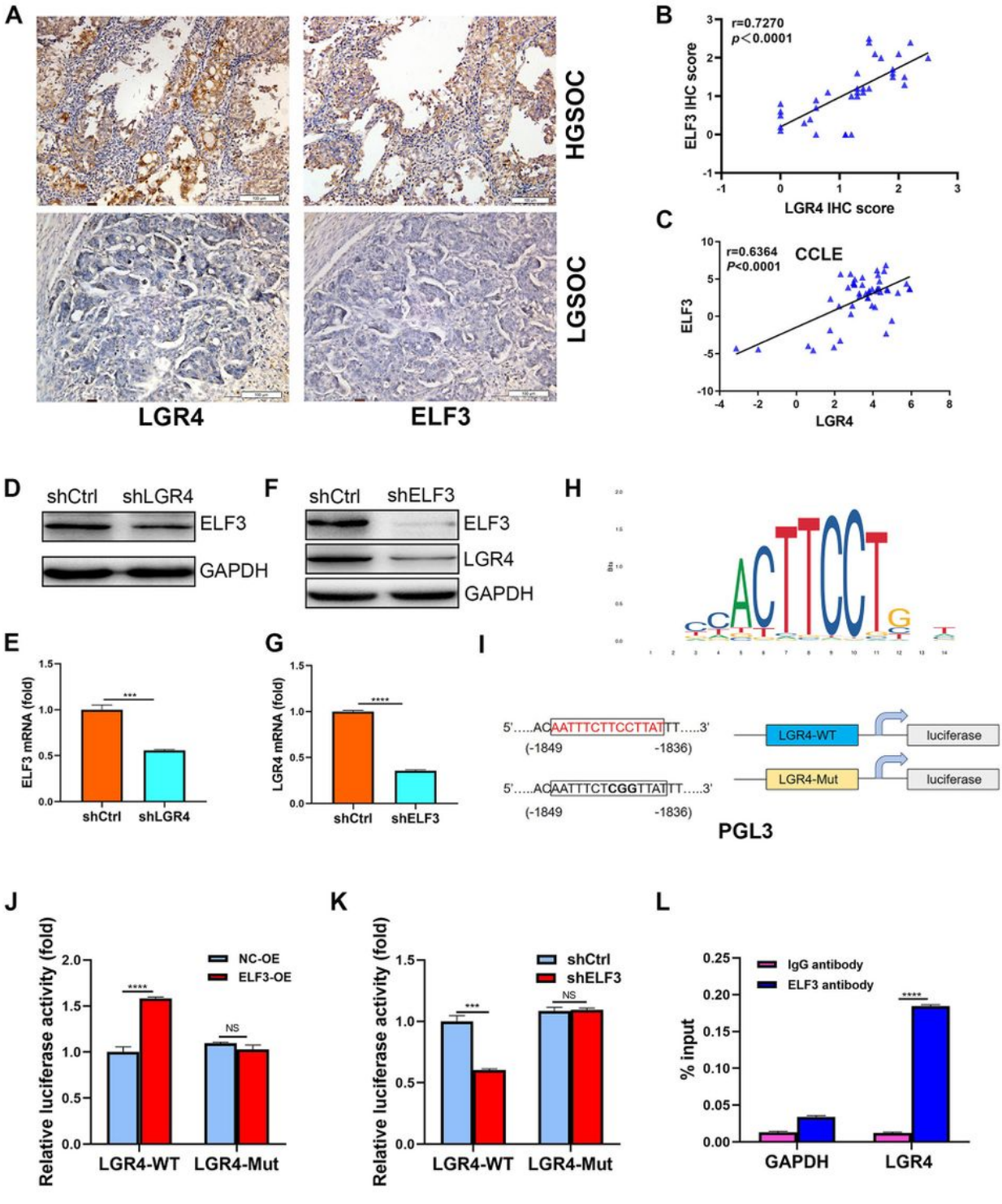

Figure 4

LGR4 and ELF3 form a reciprocal regulatory loop. (A) LGR4 and ELF3 expression was detected in the same panel of serous EOCs (n=34) by IHC. (B) LGR4 and ELF3 expression was scored, and correlation between LGR4 and ELF3 was analyzed by Pearson statistics. (C) CCLE database was interrogated for LGR4 and ELF3 expression. Correlation of LGR4 with ELF3 was analyzed by Pearson statistics. (D) and (E) ELF3 expression was detected in OVCAR3 cells transfected with Control shRNA or LGR4 shRNA by

Western blot and Real-time PCR. (F) and (G) LGR4 expression was detected in OVCAR3 cells transfected with Control shRNA or ELF3 shRNA by Western blot and Real-time PCR. (H) and (I) Wild-type (WT) and mutated (Mut) binding site sequences were shown. (J) Luciferase activity was detected in HEK293T cells transfected with Control vector or ELF3 overexpression vector. (K) Luciferase activity was detected in OVCAR3 cells transfected with Control shRNA or ELF3 shRNA. (L) ChIP and real-time PCR were performed in OVCAR3 cells. Western blot, Real-time PCR, Luciferase reporter assay and ChIP experiments were performed in triplicate. Error bars indicate SD. ***P<0.001, ****P<0.0001, NS: no significance.

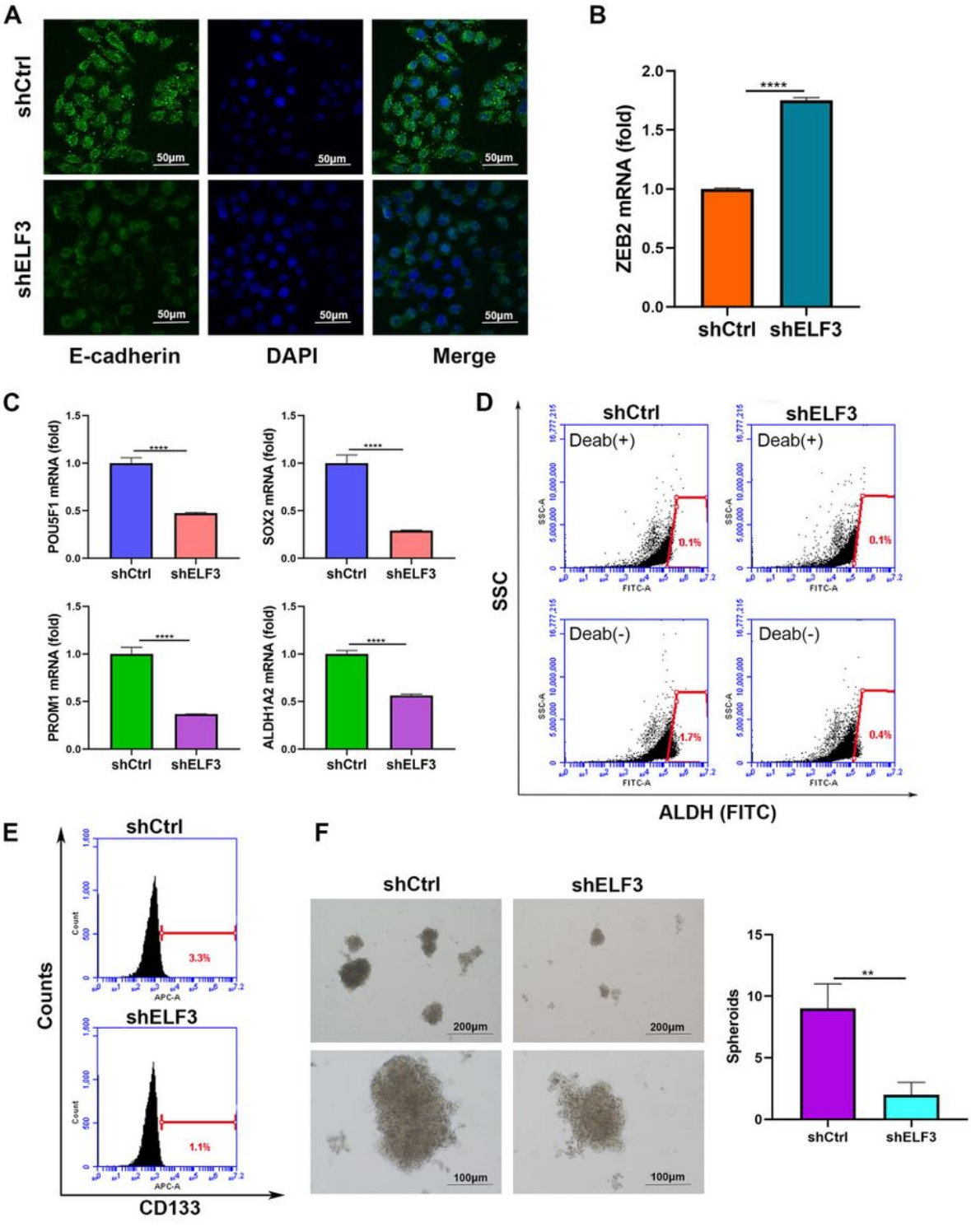

Figure 5

ELF3 is involved in HGSOC cell epithelial phenotype and stem-like traits. (A) E-cadherin expression was detected in OVCAR3 cells transfected with Control shRNA or ELF3 shRNA by Immunofluorescence. (B) ZEB2 expression was detected in OVCAR3 cells transfected with Control shRNA or ELF3 shRNA by Real-time PCR. (C) POU5F1, SOX2, PROM1 and ALDH1A2 expression was detected in OVCAR3 cells transfected with Control shRNA or ELF3 shRNA by Real-time PCR. (D) and (E) ALDH+ and CD133+ subpopulations were detected in OVCAR3 cells transfected with Control shRNA or ELF3 shRNA by Flowcytometry. (F) Spheroids per field were counted in OVCAR3 cells transfected with Control shRNA or ELF3 shRNA. All experiments were performed in triplicate. Error bars indicate SD. **P<0.01, ****P<0.0001.

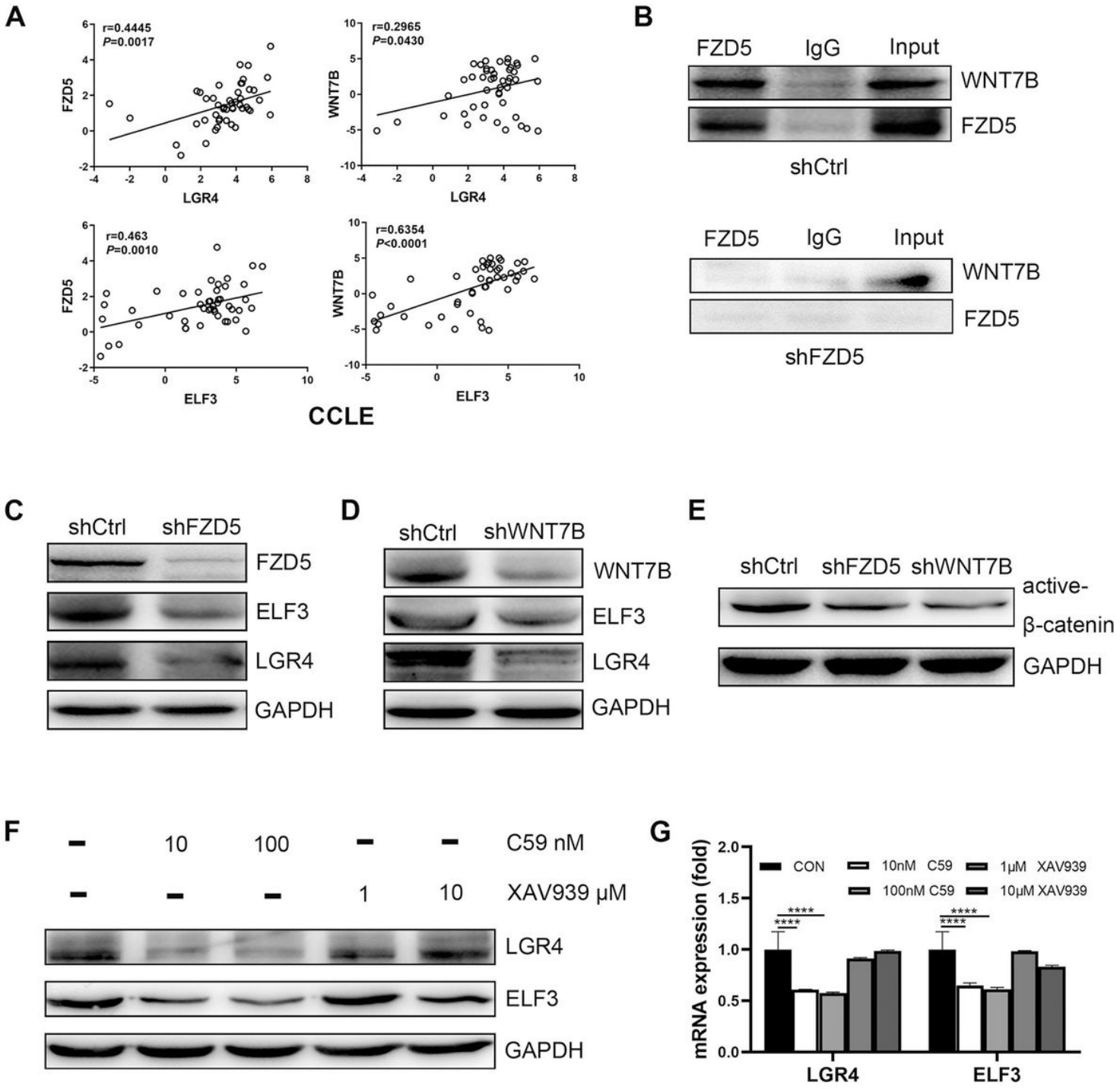

Figure 6

LGR4-ELF3 is modulated by WNT7B/FZD5 pair. (A) CCLE database was interrogated for FZD5, WNT7B, LGR4 and ELF3 expression. Correlation between two genes was analyzed by Pearson statistics. (B) Co-IP test was performed in OVCAR3 cells transfected with Control shRNA or FZD5 shRNA. (C) FZD5, ELF3, and LGR4 expression was detected in OVCAR3 cells transfected with Control shRNA or FZD5 shRNA by Western blot. (D) WNT7B, ELF3, and LGR4 expression was detected in OVCAR3 cells transfected with Control shRNA or WNT7B shRNA by Western blot. (E) Active β-catenin expression was determined in

OVCAR3 cells transfected with Control shRNA, FZD5 shRNA or WNT7B shRNA by Western blot. (F) and (G) LGR4 and ELF3 expression was detected in OVCAR3 cells treated with C59 or XAV939 by Western blot and Real-time PCR. Co-IP, Western blot, and Real-time PCR experiments were performed in triplicate. Error bars indicate SD. ****P<0.0001.

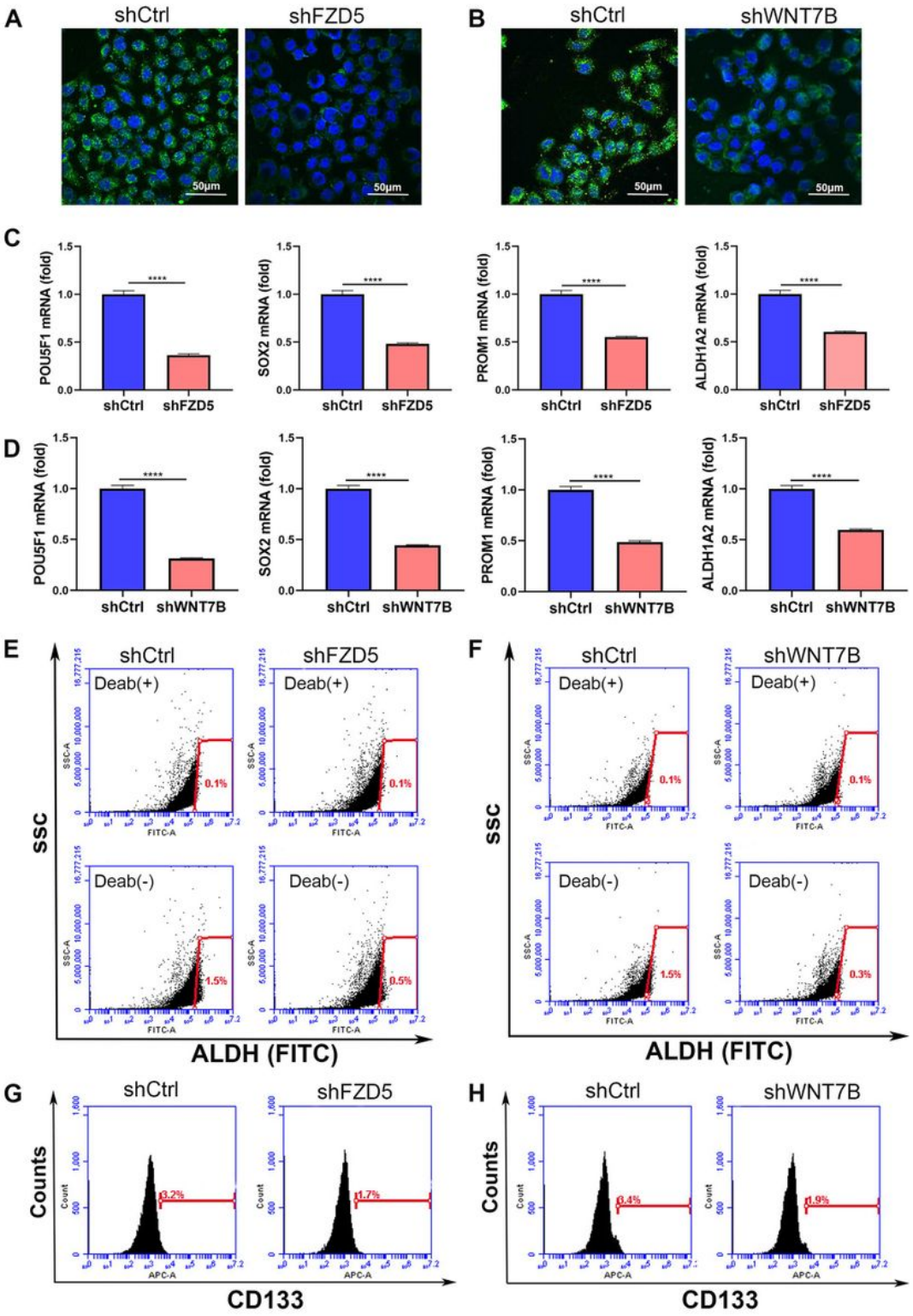

Figure 7

WNT7B/FZD5 maintains HGSOC cell epithelial phenotype and stem-like traits. (A) and (B) E-cadherin expression was detected in OVCAR3 cells transfected with FZD5 shRNA and WNT7B shRNA, respectively, by Immunofluorescence. (C) and (D) POU5F1, SOX2, PROM1 and ALDH1A2 expression was detected in OVCAR3 cells transfected with FZD5 shRNA and WNT7B shRNA, respectively, by Real-time PCR. (E) and (F) ALDH+ subpopulations were detected in OVCAR3 cells transfected with FZD5 shRNA and WNT7B shRNA, respectively, by Flowcytometry. (G) and (H) CD133+ subpopulations were detected in OVCAR3 cells transfected with FZD5 shRNA and WNT7B shRNA, respectively, by Flowcytometry. All experiments were performed in triplicate. Error bars indicate SD. ****P<0.0001.

Supplementary Files

This is a list of supplementary files associated with this preprint. Click to download.

- supplement11.tif
- supplement12.tif
- supplement13.tif
- supplement14.tif